

Electronic Supplementary Information

Scientific insight into the dual role of Cu–cocatalysts for electron injection onto schottky junctions: sunlight driven H₂ production with Cu@Si–CdS system†

Khezina Rafiq^{ab}, Muhammad Zeeshan Abid^{ac}, Khalid Aljohani^d, Bassam S. Aljohani^e, Muhammad Jalil^a, Sohaila Andleeb^f, Ejaz Hussain^{ag}*

^aInstitute of Chemistry, Inorganic Materials Laboratory 52S, The Islamia University of Bahawalpur–63100, Pakistan.

^bShimmer Center, Tianfu Jiangxi Laboratory, Chengdu, 641419, P.R. China.

^cCollege of Chemistry and Molecular Sciences, Henan University, Kaifeng, 475004, PR China.

^dDepartment of Mechanical Engineering, College of Engineering in Al-Kharj, Prince Sattam Bin Abdulaziz University, Al-Kharj, 11942, Saudi Arabia.

^eDepartment of Mechanical Engineering, College of Engineering, Taibah University, Yanbu, 41911, Saudi Arabia.

^fInstitute of Chemistry, University of Sargodha, Sargodha Pakistan.

^gInternational Center for Interdisciplinary Research in Sciences (ICIRS), The University of Lahore, Lahore, Pakistan.

Corresponding authors: ejaz.hussain@iub.edu.pk

Chemicals:

The following chemicals were used during synthesis of Cu@Si-CdS: cadmium nitrate ($\text{Cd}(\text{NO}_3)_2 \cdot 4\text{H}_2\text{O}$, 98%, CAS # 10022-68-1, Merck), sodium sulphide (Na_2S , 98%, CAS # 1313-82-2, Merck), chloroacetic acid (ClCH_2COOH , 99%, CAS # 79-11-8, Merck), Tetramethoxysilane ($\text{Si}(\text{OCH}_3)_4$), sodium borohydride (NaBH_4 , 98%, CAS # 16940-66-2, Merck), ammonia solution (NH_4OH , 28–30%, CAS # 1336-21-6, Merck) and copper nitrate ($\text{Cu}(\text{NO}_3)_2 \cdot 3\text{H}_2\text{O}$, 99%, CAS # 10031-43-3, Merck). As cited by the providers, all of the above-mentioned chemicals were specifically made for the synthesis of the catalyst and the photoreaction procedure. All solutions were made with double-distilled water.

Instruments:

A specifically designed autoclave made of stainless-steel (to prevent any corrosion) lined with Teflon (Technistro) was used for hydrothermal reaction. Synthesis was carried out in a heating oven (SANFA DHG-9030). Sonication (Elma Schrnidbauer GmbH, D-78224 Singen, Germany) was used to disseminate the as-synthesized nanoparticles. A Vulcan A-130 furnace was used for calcination.

XRD patterns were obtained using Bruker D2 PHASER XE-T which is a commonly used instrument to get information of structural morphology of as-synthesized photocatalysts¹. In that instrument, a specifically designed single chroma digital approach was used, that helped to obtain a high energy resolution of 380 eV to ensure the high precision of results². The reason for choosing this approach was that it filter out any undesired sources of radiation that could reduce the precision of the process³. The structuration of its powder was examined using scanning electron microscopy via Nova-Nano SEM equipped with EDX (Energy-dispersive X-ray spectroscopy) features⁴. Various spectrometers are available for determining optical properties of a material. One

of them is a UV-VIS-based Perkin Elmer-LAMBDA-850⁵. This was used in this study to determine the optical properties of CdS by setting the spectral range between 300 and 800 nm⁶. Moreover, for monitoring of experiments in dye degradation of this photocatalyst, the same instrument was used.

An instrument named “Kratos Axis Ultra-DLD was used to acquire the X-ray photoelectron spectroscopy characterization details ⁷. A Solatron impedance analyzer was used for the electrochemical impedance spectroscopy analysis. Furthermore, to perform photocurrent tests, a tri-electrode system was used with the help of a potentiostat and visible light, utilizing a CH instruments CHI 660 instrument ⁸.

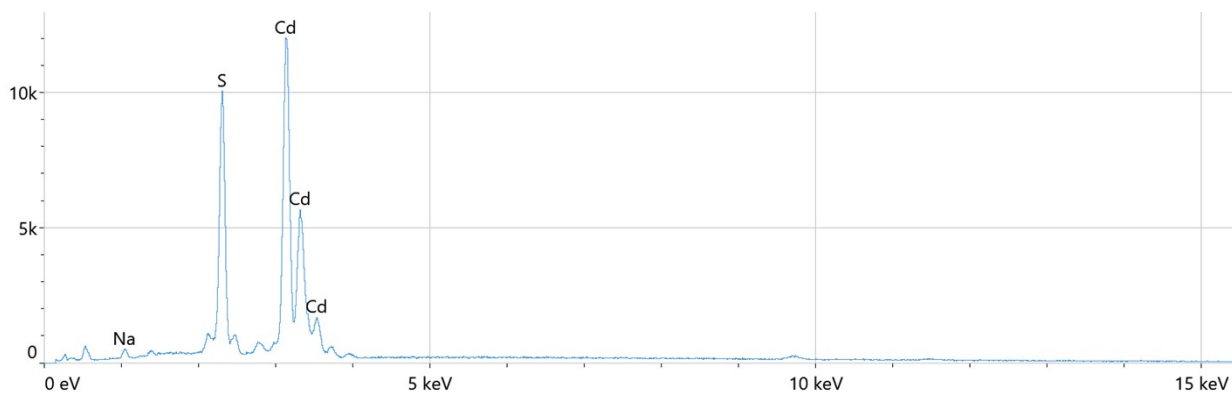


Fig. S1: EDX analysis of pristine CdS.

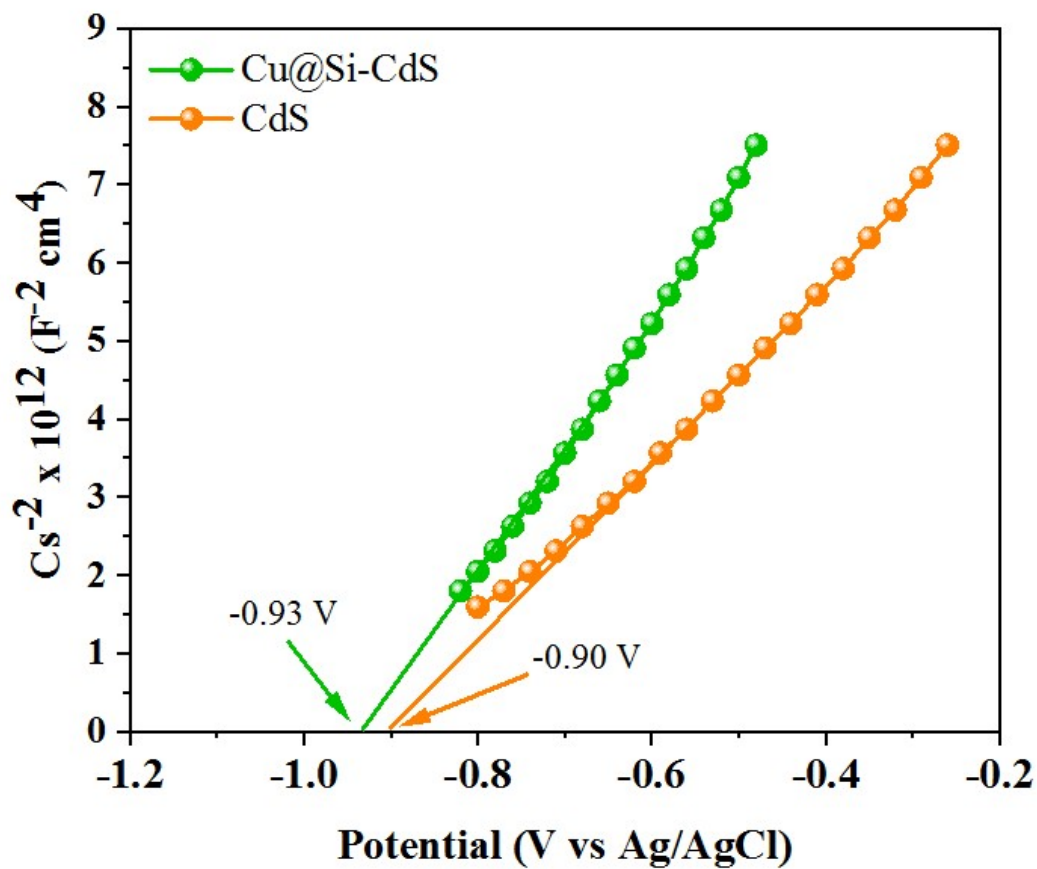


Fig. S2: Mott schottky plot of CdS, and Cu@Si-CdS photocatalysts.

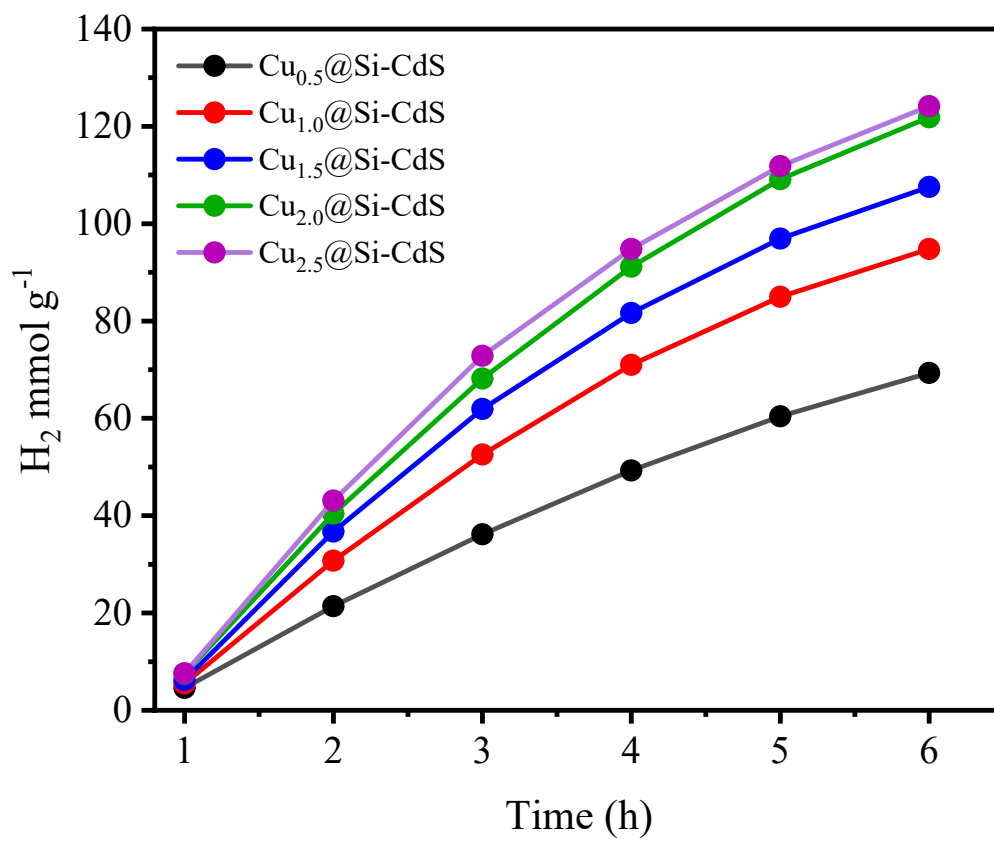


Fig. S3: Activities of catalysts for the optimization of Cu metal loading.

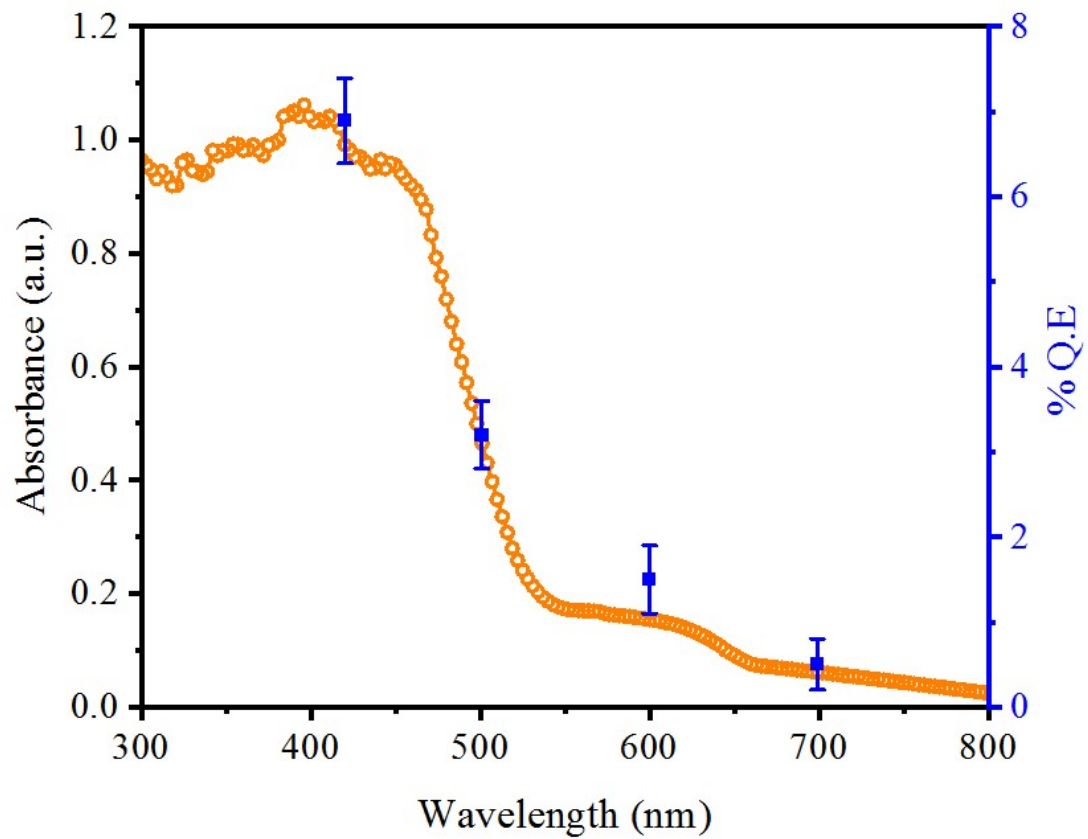


Fig. S4: Wavelength dependent activities of the catalyst.

Factors affecting the progress of photoreaction:

The band gap of a photocatalysts is a critical factor influencing its performance for hydrogen generation. The band gap represents the energy difference between the valence and conduction bands of a semiconductor. For efficient water splitting, the valence band potential of a photocatalysts must be more positive than the oxidation potential of O_2/H_2O , while its conduction band potential must be more negative than the reduction potential of H_2O/H_2 . Catalysts with a band gap of 3.2 eV or higher can only split water when exposed to UV irradiation and are ineffective for hydrogen evolution in visible light. To enhance performance under visible light, reducing the band gap is essential, that is usually achieved through metal loading or doping. In this study, Si metal doping reduced the band gap of CdS from 3.2 eV to 2.9 eV that helped to achieve a more suitable band gap for hydrogen evolution in visible light. Si–CdS exhibited greater hydrogen production compared to bare CdS due to the difference in band gap energy⁹. These findings emphasize the critical role of band gap reduction, achieved through Si metal doping, to enhance the efficiency of CdS photocatalysts for hydrogen generation under visible light. In addition to band gap, other factors such as light intensity, surface area, pH, temperature, photocatalysts dosage, and the presence of sacrificial agents can also influence the performance of photocatalysts for hydrogen generation.

Band gap:

Band gap is one of the most important factors, as it determines the wavelengths of light that can be absorbed by the photocatalysts and the energy available for driving the water splitting reaction. In current study, Band gap has been tuned with Si dopants and Cu cocatalysts. By manipulating the band gap of CdS photocatalysts through Cu@Si–CdS, researchers have developed a promising new technology for efficient hydrogen production under visible light.

pH:

pH of any solution is concentration of H^+ ions or OH^- ions. It directly influences the rate of hydrogen evolution¹⁰. The conversion of photons to the hydrogen is highly smoothed by the presence of photons which serve as electron acceptors, and react with the electrons. Another point to notice is that, acidity or basicity of a media also affects the speed at which H_2 is evolved. The process is facilitated in a faintly basic medium having pH of 9. This medium has shown the best results of H_2 evolution of $24.92 \text{ mmol g}^{-1} \text{ h}^{-1}$ see results in the [Fig.9a](#).

The severity on either lower or higher side of temperature could decrease the evolution rate of H_2 . The phenomenon can be said to due to inverse effect of a media being on low of high side of the pH, ultimately reducing the activity of the photocatalysts in hydrogen evolution. As a result, the above-mentioned conditions of pH of 9 were established for our experiment.

Temperature:

The effect of temperature on the process is not as much as that of the other factors. This is because the temperature does not necessarily cause the induction of electrons for H_2 generation thermodynamically¹⁰. But there is one thing for which it plays an important role and that is stripping of the reactive products from the face of the catalyst. This process of stripping is directly proportional to the temperature; hence increased temperature can definitely enhance the hydrogen generation process. In contrast, lower temperatures slow down the desorption process, causing products to accumulate on the photocatalysts surface. We can say that high temperature can do following goods to our process. Accelerated transfer of electrons from valence band to the conduction band increased vapor pressure. Increased efficiency of photoreactions¹¹.

The hydrogen evolution rate in our process was found to be $25.27 \text{ mmol g}^{-1} \text{ h}^{-1}$ at $35 \text{ }^\circ\text{C}$ at pH 9 see [Fig. 9b](#). This was found to be the optimal temperature for our process. Something worth noting is

that increased temperature can severely alter the constancy and structuration of the catalysts. Moreover, a very low amount of H₂ is produced in those processes which did not went through calcination. The variations in temperature of calcination can cause variations in size and morphology of the catalyst.

Catalysts Concentration:

Just like the other factors mentioned before, the concentration of Cu@Si–CdS catalysts has also evolved as a crucial factor in influencing the activity. Increasing the concentration of photocatalysts resulted in a greater exposure to sunlight, leading to the production of more electrons and, consequently, higher hydrogen evolution rates¹². However, it was observed that beyond an optimized concentration, the photocatalysts activity began to decline. This decline was attributed to the excessive concentration of photocatalysts causing particle agglomeration, which hindered the penetration of sunlight. Specifically, at higher concentrations, the particles tended to aggregate and block the irradiation of sunlight. In our study, the optimum value of H₂ production was 25.28 mmol g⁻¹ h⁻¹. This optimum value was achieved at a dose of 20 mg of our catalyst at 35°C and pH 9 see [Fig. 9c](#). In contrast, when the dose of the catalyst was doubled, a slightly higher but still limited hydrogen production was noticed ¹³.

Intensity of light:

The photocatalytic hydrogen generation process was conducted under natural sunlight conditions, where the activity of the photocatalysts was observed to be directly affected by the concentration of light. The mean value of light intensity of the sun that falls on the face of the earth is more than 1300 W/m². The intensity of light hitting the surface of earth in the morning is comparatively low. Hence, the hydrogen evolution rate was also low. However, after the early hours of the day, rate

increased significantly as a result of the higher light intensity directly illuminating the photocatalysts. Similarly, the rate also decreased in the afternoon hours once the sunlight started diminishing. Multiple experiments were conducted to investigate the impact of sunlight intensity on photocatalytic activity, revealing a direct correlation between increased light intensity and higher hydrogen-evolution rates¹⁴. As depicted in the highest hydrogen evolution, measuring 25.21 mmol g⁻¹ h⁻¹, was achieved under sunlight irradiation with an intensity of 700 W/m² using 20 mg catalysts at 35°C and pH 9 see [Fig. 9d](#).

Role of the sacrificial reagent:

Water splitting is a technique where various photocatalysts are used, but there many down sides of using them. One of the major hurdles in using photocatalysts is that the holes and electrons start to recombine in this development. Sacrificial agents are ones which are used to lessen this recombination process. The electrons absorb energy to change to the conduction band. There, they are used for hydrogen generation through the reduction of Hydrogen Oxide. While this process is ongoing, the sacrificial agents speedily absorb the holes and get oxidized¹⁵.

To enhance the efficiency of the absorption of priority of charge carrier, sacrificial reagents such as Ag⁺, Fe³⁺, and Ce⁴⁺ can be employed for oxidizing water by accepting electrons, thereby promoting oxygen gas production. Additionally, electron donors like C₂H₅OH, CH₃OH, 2-hydroxypropanoic acid, triethanolamine, cyanide, EDTA, Na₂SO₃, and Na₂S can be utilized in the process of consumption of holes. This resultantly generates the desired H₂ gas. C₂H₅OH and CH₃OH are two of the most effectively used sacrificial reagents.

For this study, 5% ethyl alcohol solution in water was used to act as a sacrificial reagent for following reasons. It is more cost effective. It can easily be obtained from renewable resources. It can easily lead to the production of products that would be oxidized, by consuming holes. 5% ethyl

alcohol is an optimum concentration¹⁶. Although the increased concentration of sacrificial reagent increased the production of hydrogen, but it can saturate catalyst's surface very quickly and hence hindering its activity.

References

1. C. Moczygemba, J. George, E. Montoya, E. Kim, G. Robles and E. Sooby, *Journal of Nuclear Materials*, 2022, 570, 153951.
2. Y. Wu, J. Ma, P. Su, L. Zhang and B. Xia, *Nanomaterials*, 2020, 10, 2482.
3. C. Lauro, L. C. Brandao, D. Baldo, R. Reis and J. Davim, *Measurement*, 2014, 58, 73-86.
4. N. Thakur, K. Kumar, V. K. Thakur, S. Soni, A. Kumar and S. S. Samant, *Nanofabrication*, 2022, 7, 62-88.
5. T. Germer, J. C. Zwinkels and B. K. Tsai, *Spectrophotometry: Accurate measurement of optical properties of materials*, Elsevier, 2014.
6. M. Mahdi, Z. Hassan, S. Ng, J. Hassan and S. M. Bakhori, *Thin Solid Films*, 2012, 520, 3477-3484.
7. G. Greczynski and L. Hultman, *Journal of Applied Physics*, 2022, 132.
8. X. Xu, G. Liu, S. Ni and J. T. Irvine, *Journal of Physics: Energy*, 2018, 1, 015001.
9. J. A. Nasir, Z. ur Rehman, S. N. A. Shah, A. Khan, I. S. Butler and C. R. A. Catlow, *Journal of Materials Chemistry A*, 2020, 8, 20752-20780.
10. X. Tian, P. Zhao and W. Sheng, *Advanced Materials*, 2019, 31, 1808066.
11. M. Sabir, K. Rafiq, M. Z. Abid, U. Quyyum, S. S. A. Shah, M. Faizan, A. Rauf, S. Iqbal and E. Hussain, *Fuel*, 2023, 353, 129196.
12. B. Bakbolat, C. Daulbayev, F. Sultanov, R. Beissenov, A. Umirzakov, A. Mereke, A. Bekbaev and I. Chuprakov, *Nanomaterials*, 2020, 10, 1790.
13. P. Zhang, L. Feng, B. Su and X. Li, *Journal of Cleaner Production*, 2022, 341, 130895.
14. Y. Jiang, Z. Sun, C. Tang, Y. Zhou, L. Zeng and L. Huang, *Applied Catalysis B: Environmental*, 2019, 240, 30-38.
15. Z. Rao, G. Lu, L. Chen, A. Mahmood, G. Shi, Z. Tang, X. Xie and J. Sun, *Chemical Engineering Journal*, 2022, 430, 132766.
16. V. Kumaravel, M. D. Imam, A. Badreldin, R. K. Chava, J. Y. Do, M. Kang and A. Abdel-Wahab, *Catalysts*, 2019, 9, 276.